

Influence of the Boundary Conditions on the Outlet for Numerical Simulation of the Stratified Flow Over the Hill

L. Beneš¹

Summary: *The article deals with the numerical simulation of the stratified incompressible flows over the isolated hill. The mathematical model is based on the Boussinesq approximation of the Navier–Stokes equations for viscous incompressible flow with non-constant density. The resulting set of PDE's is then solved by the AUSM MUSCLE scheme in finite volume approximation. For the time integration the three stage BDF method of the second order is used. The simulation was performed for the wide range of Ri numbers. For $Ri = 0.5$ three different boundary conditions on the outlet are tested.*

Keywords: Stratified flow, AUSM MUSCL, Variable density

1. Introduction

Influence of the stratification is significant in many processes taking place in ABL (e.g. stratification affects the transport of pollutants, plays significant role in determining the consequences of accidents on environment and human etc.). Stratified flows in environmental applications are characterized by the variation of fluid density in the vertical direction that can lead to appearance of specific phenomena which are not present when density is constant, namely internal and gravity waves. The beginning of the studies of internal waves, produced by a flow over topography or body, moving in stratified liquid, is dating back to XIX century and is still continuing. The experimental and numerical studies of the generation of the gravity waves were proposed by e.g. (1),(2),(3),(4).

From the numerical point of view, the simulations of stratified fluid flows are in general more demanding than the solution of similar non-stratified flow cases. The system of equations involves one additional transport equation in comparison to the non-stratified case. The transport equation for the density (or its perturbation as in our case) is coupled to momentum equations by a buoyancy term. Because of this buoyant force the obstacles in flow generate waves. These waves propagate at long distances from the obstacle. Its frequency depends on the level of the stratification. The correct resolution of the gravity waves is sensitive on the numerical viscosity. Other question is influence of the boundary conditions on the artificial boundaries of the computational domain. Both of this questions are tested in our contribution.

Since of 2000 we deal with the numerical study of the ABL flows (flow over open coal mine, Prague region, Giant mountains). In these studies we have supposed that the ABL is neutrally

¹ Doc. Ing. Luděk Beneš PhD Dept. Of Technical Mathematics, Faculty of Mechanical Engineering, Czech Technical University in Prague, Karlovo nám 13, 121 35, Prague 2, tel. +420 224357543, e-mail benes@marian.fsik.cvut.cz

stratified. The stratified flow we have studied since 2008. The first studies was devoted to the simulation of the flow past a ball in 2D (9) using WENO, AUSM MUSCL and compact differences schemes . The extension to 3D was published in (8). Next studies were devoted to the flow around thin vertical strip (10) and over sinusoidal hill (6).

2. Mathematical model

The fluid in the ABL is assumed to be incompressible, yet the density is not constant due to gravity. This type of flow can be described by the Navier-Stokes equations for viscous incompressible flow with variable density. These equations are simplified by the Boussinesq approximation. Density and pressure are divided into two parts: a background field (with subscript $_0$) plus a perturbation. The system of equations obtained is partly linearized around the average state ρ_* . The resulting set of equations can be written in the form

$$\frac{\partial \varrho}{\partial t} + \frac{\partial(\varrho u_j)}{\partial x_j} = -u_2 \frac{\partial \varrho_0}{\partial x_2}, \quad (1)$$

$$\frac{\partial u_i}{\partial t} + \frac{\partial(u_j u_i)}{\partial x_j} + \frac{1}{\rho_*} \frac{\partial p}{\partial x_i} = \nu \frac{\partial^2 u_i}{\partial x_j \partial x_j} - \delta_{i,2} g, \quad (2)$$

$$\frac{\partial u_j}{\partial x_j} = 0, \quad (3)$$

where $W = [\varrho, u_1, u_2, p]^T$ is the vector of unknowns, $\varrho(x_1, x_2, t)$ denotes the perturbation of the density and u_1, u_2 are the velocity components, p stands for the pressure perturbation and g for the gravity acceleration. The x_1 -axis is orientated in the direction of the motion and the x_2 -axis is perpendicular to the ground.

For the description of the stratified flows with characteristic velocity U and characteristic length L following similarity numbers have been used:

$$Re = \frac{UL}{\nu}, \quad Ri = -\frac{g}{\rho_*} \frac{\frac{\partial \varrho_0}{\partial x_2}}{U}. \quad (4)$$

3. Numerical scheme

For numerical simulation of the flow over the hill, the AUSM MUSCL scheme in the finite volume formulation has been used. This scheme was successfully used in our previous computations on the similar geometries. In these cases was validated by comparison to the WENO scheme combined with the projection method and the compact finite-difference scheme. The schemes have been successfully used for simulation of the flow field around moving bodies in 2D and 3D stratified fluid for wide range of Richardson numbers see (8), (9), (10).

The scheme is based on the artificial compressibility method in dual time. The continuity equation (3) is modified and takes the form

$$\frac{\partial p}{\partial \tau} + \beta^2 \frac{\partial u_j}{\partial x_j} = 0, \quad (5)$$

where τ is the artificial time.

The spatial semidiscretization of the inviscid fluxes is achieved by the finite volume AUSM scheme. Quantities $(q)_{L/R}$ on the cell faces are computed using the MUSCL reconstruction with the Hemker-Koren limiter(12) The scheme is stabilized according to (7) by the pressure diffusion.

$$\left(0, 0, 0, \eta \frac{p_{i+1,j} - p_{i,j}}{\beta_x}\right)^T \quad \beta_x = w_r + \frac{2\nu}{\Delta x}$$

where w_r is reference velocity (in our case the maximum velocity in flow field).

The viscous fluxes are discretized using central approach on a dual mesh (diamond type scheme).

The spatial discretization results in a system of ODE's solved by the second-order BDF formula

$$\frac{3W^{n+1} - 4W^n + W^{n-1}}{2\Delta t} + L^{n+1} = 0. \quad (6)$$

Here, L^{n+1} denotes the numerical approximation of the convective and viscous fluxes described above and the source terms. Arising set of nonlinear equations is then solved by the artificial compressibility method in the dual time τ by the explicit 3-stage second-order Runge-Kutta method.

4. Computational setup

As the simplest model case was chosen flat terrain with the sine-shaped hill. The domain has dimensions $90 \times 30 m$ with hill $h = 1m$ height.

The background density field is linearly distributed with $\rho_0(x_2) = \rho_w + \gamma x_2$, $\rho_w = 1.2 kg \cdot m^{-3}$ and $\gamma = -0.01 kg \cdot m^{-4}$, the viscosity $\nu = 0.001$. In the presented paper, the flow for wide range of $Re \in < 0; 2 >$ is simulated. Then, for $Re = 0.5$ the influence of the outlet boundary conditions on the generation of the gravity waves was tested. The level of the stratification isn't changed by the changing of the density gradient but by the modification of the gravity constant.

The computations have been performed on structured non-orthogonal grid. The grid consist of 233×117 points refined near the ground and in the vicinity of the hill. The minimal resolution in the x_2 direction is $\Delta x_2 = 0.03m$.

The following boundary conditions are satisfied. On the inlet the velocity profile is given by the relation $u_1(x_2) = U_0(x_2/H)^{1/r}$ where $U_0 = 1m/s$ and $r = 40$ was prescribed, $u_2 = 0$, $\rho = 0$ and pressure perturbation is extrapolated. Homogeneous Neumann conditions for all quantities are satisfied on the top. No-slip boundary conditions for the velocity components and homogeneous boundary conditions for pressure and density perturbations are prescribed on the ground. The three different boundary conditions are prescribed on the outlet.

- BC1:** homogeneous Neumann condition are prescribed for velocity components and pressure perturbations. Pressure is set zero (homogeneous Dirichlet b.c.).
- BC2:** advection equation $\frac{\partial q}{\partial t} + U_a \frac{\partial q}{\partial x} = 0$ is satisfied for $q = u_1, u_2, \rho$, pressure is extrapolated. The advection velocity U_a is computed as the mean value of the u_1 velocity on the inlet.
- BC3:** are similar to previous case, only pressure is set zero.

The computations have been performed on structured non-orthogonal grid. The grid consists of 233×117 points refined near the ground and in the vicinity of the hill. The minimal resolution in the x_2 direction is $\Delta x_2 = 0.03m$.

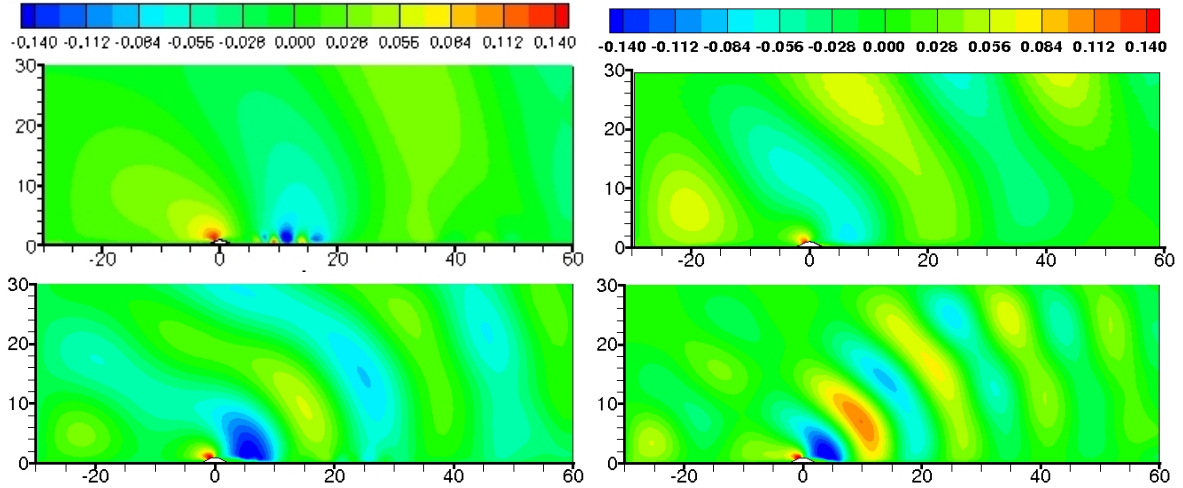


Figure 1: Isolines of the u_2 -velocity component for $Ri = 0.2, 0.5, 1, 2, BC1$.

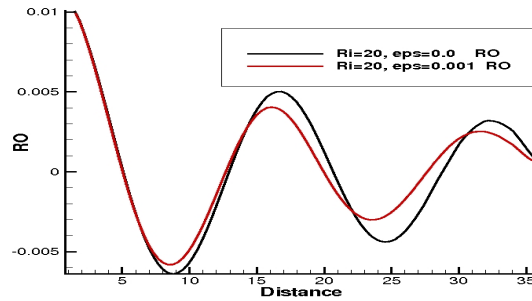


Figure 2: Dependence of the gravity waves on the pressure diffusion term (right).

5. Numerical results

Fig. 1 displays the dependence of the flow on the level of stratification. A comparison of the isolines of the u_2 -velocity component for four different Richardson numbers ($Ri = 0.2, 0.5, 1, 2$) is presented at the same time. The gravity waves with the wavelength given by the Brunt-Väisälä frequencies are visible. The presented simulations are affected by some non-physical artifacts related to the implementation of the boundary conditions on the artificial boundaries of the computational domain. Most pronounced is the wave pattern located close to the lower left corner of the domain. This effect is generated by the inlet velocity profile and is local in the non-stratified case. In stratified one this perturbation generates the second system of gravity waves.

Fig. 2 demonstrates sensitivity of the gravity waves on the artificial diffusion in the scheme. Relatively small pressure diffusion leads not only to dumping of the waves but also to changes in its frequency.

Fig. 3 displays the dependence of the flow on the boundary conditions. A comparison of the isolines of the u_2 -velocity component for BC1 – BC3 is presented at the same time. The parasitive wave structure on the inlet is strongest in the case BC3. The values of u_2 ranges for BC1,2 in $u_2 \in \langle -0.228, 0.206 \rangle$, for BC3 in $u_2 \in \langle -0.154, 0.207 \rangle$. Similarly also density perturbations are lower in BC3 case ($\rho \in \langle -0.0065, 0.0165 \rangle$ BC1,2, $\rho \in \langle -0.0044, 0.0120 \rangle$ BC3). The 'bean' structure of the waves is given by the reflection from the upper boundary.

The BC1 and BC2 produce practically the same results. It is clearly visible in the Fig.4

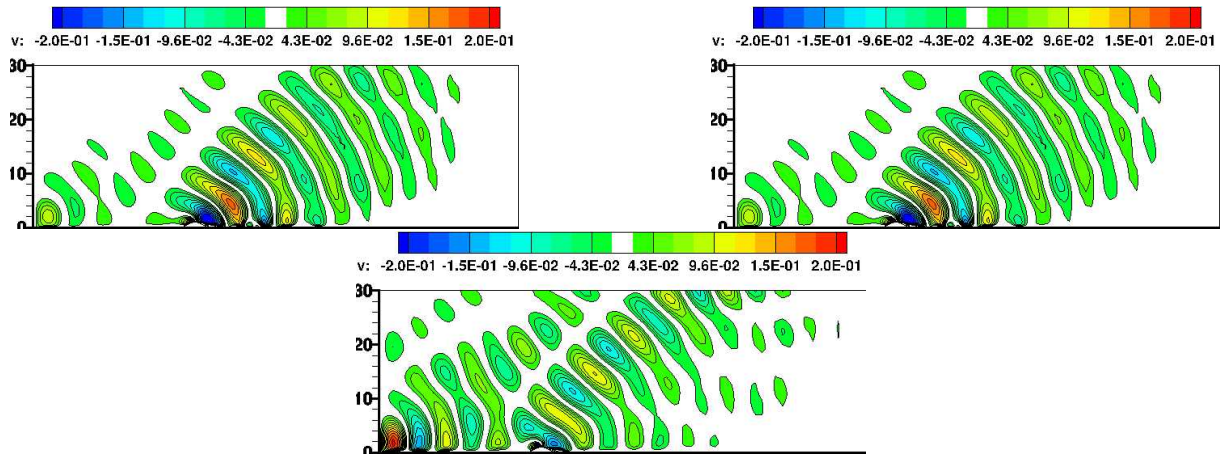


Figure 3: Gravity waves pattern for three different boundary conditions. BC 1 – top left, BC 2 – top right, BC 3 – bottom.

where the relative error of the density perturbation ρ and u_2 -velocity component is shown. The differences are very small and are concentrated close to the ground behind the hill. On the other hand, BC3 generates different results. The waves on the inlet are significantly stronger in this case. Relative error to the BC1 case is shown in Fig.5. The differences are mainly close to the ground and in front of the hill. Also position of the waves are shifted.

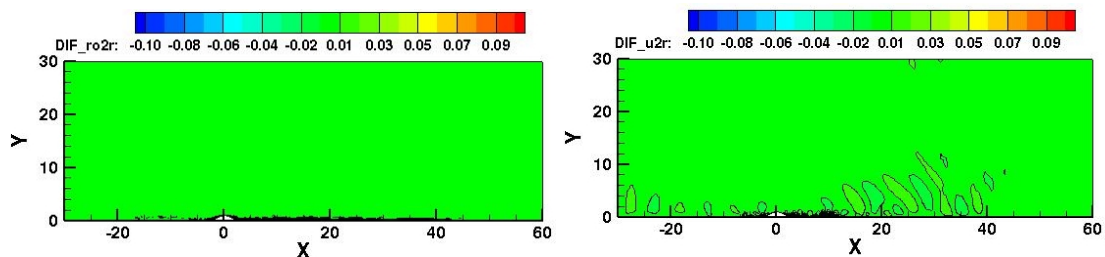


Figure 4: Relative differences of the density perturbation ρ (left) and u_2 -velocity component (right). Case BC1-BC2.

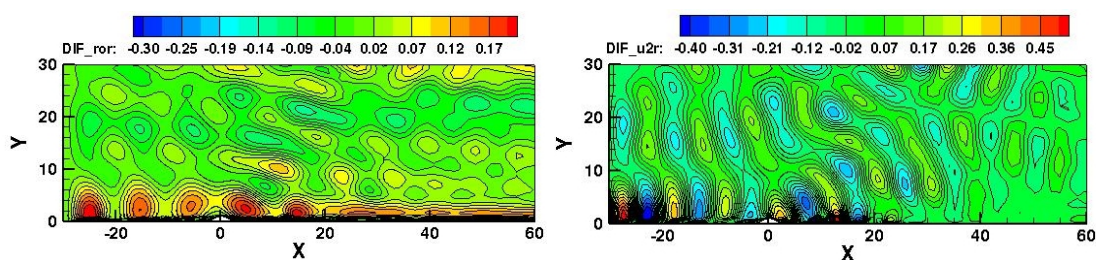


Figure 5: Relative differences of the density perturbation ρ (left) and u_2 -velocity component (right). Case BC1-BC3.

6. Conclusion

The flow over the hill in the stratified fluid was simulated. Three different outlet boundary conditions were implemented and compared.

Presented results show suitability of the scheme for modeling of this type of problems. The flow was significantly influenced by the boundary condition for pressure on the outlet. The

improvement of the upper boundary conditions is necessary. The gravity waves crossing this boundary and homogeneous Neumann condition for all quantities isn't fully valid.

For the deeper understanding of the behavior of these models and boundary conditions further research is necessary.

Acknowledgments: This work was supported by TACR Project TA01020428 and grant CTU SGS13/174/OHK2/3T/12.

7. References

- [1] Boyer D., Davies P., Fernando H., Zhang X.: Linearly stratified flow past a horizontal circular cylinder. *Phil. Trans. R. Soc. Lond.* **A328**, 501-528, 1989.
- [2] Hanazaki H., Kashimoto K., Okamura T.: Jets generated by a sphere moving vertically in a stratified fluid. *J. of Fluid Mech.* **638**, 173–197, 2009
- [3] Sutherland B., Linden P.: Internal wave excitation from stratified flow over a thin barrier. *J. Fluid. Mech.* **377**, 223-252, 1998.
- [4] Castro I.: Weakly stratified laminar flow past normal flat plates. *J. Fluid Mech.* **454**, 21-46, 2002.
- [5] Bodnár T., Beneš L., Fraunié Ph., Kozel K.: Application of compact finite–difference schemes to simulations of stably stratified fluid flows. *Applied Mathematics and Computation*, in press, DOI:10.1016/j.amc.2011.08.058 .
- [6] T. Bodnár, L. Beneš, Ph. Fraunié, K. Kozel Application of compact finite-difference schemes to simulations of stably stratified fluid flows. *Applied Mathematics and Computation* doi:10.1016/j.amc.2011.08.058 Article in press.
- [7] Dick E., Vierendeels J., Rienslagh K.: A multigrid semi–implicit line–method for viscous incompressible and low–mach–number flows on high aspects ratio grids. *Journal of Computational Physics* **154** 310–341 (1999)
- [8] Beneš L., Fürst J.: Numerical simulation of the Stratified Flow Past a Body. *Numerical Mathematics and Advanced Applications. ENUMATH 2009*. Berlin: Springer, 2010, p. 155-162. ISBN 978-3-642-11794-7.
- [9] Beneš L., Fürst J., Fraunié Ph.: Numerical simulation of the stratified flow using high order schemes. *Engineering Mechanics*, 16(1):39–48, 2009. ISSN 1210-2717.
- [10] Beneš L., Fürst J., Fraunié Ph.: Comparison of two numerical methods for the stratified flow. *J. Computers & Fluids*, in press, doi:10.1016/j.compfluid.2011.02.003.
- [11] Berrabaa S., Fraunié Ph., Crochet M.: 2D Large Eddy Simulation of Highly Stratified Flow: The Stepwise Structure Effect. *Advances in Computation: Theory and Practise*, **7**, 179–186, 2001. Nova Sc. Publishers.
- [12] Hemker P.W., Koren B.: Multigrid, defect correction and upwind schemes for the steady Navier-Stokes equations. *Numerical methods for fluid dynamics III; Clarendon Press/Oxford University Press*, 1988, p. 153-170.